

Title Page

Pharmacologic inhibition of Mnks in acute myeloid leukemia

Theodosia Teo, Frankie Lam, Mingfeng Yu, Yuchao Yang, Sunita KC Basnet, Hugo Albrecht, Matthew J Sykes, and Shudong Wang

Centre for Drug Discovery and Development, Sansom Institute for Health Research, Centre for Cancer Biology, and School of Pharmacy and Medical Sciences, University of South Australia, Adelaide, South Australia 5001, Australia.

Running title

MAPK-interacting kinase inhibition in AML

Corresponding Author

Shudong Wang

Address: Centre for Drug Discovery and Development, School of Pharmacy and Medical Sciences, University of South Australia, Adelaide, South Australia 5001, Australia

Tel.: +61 8 830 22372; Fax: +61 8 830 21087

E-mail: shudong.wang@unisa.edu.au

Number of text pages: 21

Number of tables: 2

Number of figures: 4

Number of references: 59

Number of words in the *Abstract*: 246

Number of words in the *Introduction*: 750

Number of words in the *Discussion*: 1500

List of non-standard abbreviations

4E-BP, eukaryotic initiation factor 4E-binding protein; Akt, Ak thymoma; AML, acute myeloid leukemia; Bcl-2, B-cell lymphoma-2; Bcr-Abl, breakpoint cluster region-abelson; CDK, cyclin-dependent kinase; eIF, eukaryotic initiation factor; ERK, extracellular-signal-regulated kinase; FAB, French-American-British classification system; FACS, fluorescence-activated cell sorting; FITC, fluorescein isothiocyanate; FLT3, feline McDonough sarcoma-like tyrosine kinase-3; GI₅₀, 50% growth inhibitory concentration; ITD, internal tandem duplications; MAPK, mitogen-activated protein kinase; Mcl-1, myeloid cell leukemia-1; Mnk, mitogen-activated protein kinase-interacting kinase; mTOR, mammalian target of rapamycin; PARP, poly(ADP-ribose)polymerase; PI, propidium iodide; PI3K, phosphatidylinositol 3-kinase; Pim-1, provirus integration site for Moloney murine leukemia virus-1; Raf, rapidly accelerated fibrosarcoma; Ras, rat sarcoma; Rb, retinoblastoma protein; RNA, ribonucleic acid; rpS6, ribosomal protein; SD, standard deviation; Tb, terbium; WT, wild-type

Abstract

The Ras/Raf/MAPK and PI3K/Akt/mTOR pathways are key signaling cascades involved in the regulation of cell proliferation and survival, and have been implicated in the pathogenesis of several types of cancers, including AML. The oncogenic activity of eIF4E driven by Mnk kinases is a convergent determinant of the two cascades, suggesting that targeting the Mnk/eIF4E axis may provide therapeutic opportunity for the treatment of cancer. Herein, a potent and selective Mnk2 inhibitor MNKI-85, and a dual-specific Mnk1 and Mnk2 inhibitor MNKI-19, both derived from a thienopyrimidinyl chemo-type, were selected to explore their anti-leukemic properties. MNKI-19 and MNKI-85 are effective in inhibiting the growth of AML cells which possess an M5 subtype with FLT3-ITD mutation. Further mechanistic studies show that the downstream effects with respect to the selective Mnk1/2 kinase inhibition in AML cells causes G₁ cell cycle arrest followed by induction of apoptosis. MNKI-19 and MNKI-85 demonstrate similar Mnk2 kinase activity and cellular anti-proliferative activity, but exhibit different time-dependent effects on cell cycle progression and apoptosis. Collectively, this study shows that pharmacologic inhibition of both Mnk1 and Mnk2 can result in a more pronounced cellular response than targeting Mnk2 alone. MNKI-85, a first-in-class inhibitor of Mnk2, however, can be used as a powerful pharmacologic tool in studying the Mnk2/eIF4E-mediated tumorigenic mechanism. In conclusion, this study provides a better understanding of the mechanism underlying the inhibition of AML cell growth by Mnk inhibitors and suggests their potential utility as a therapeutic agent for AML.

Introduction

Acute myeloid leukemia is a genetically heterogeneous cancer characterized by a collection of mutations and chromosomal translocations in immature myeloid cells that cooperate to interrupt the proliferative or survival pathways (Gilliland et al., 2004). The aberrant fusion transcription factors expressed in myeloid cells can impair hematopoietic differentiation; however, single genetic alteration is insufficient to induce leukemogenesis in most cases (He et al., 1997; Yuan et al., 2001). Particularly, constitutively activated signal transduction pathways derived from the mutated genes that normally regulate hematopoietic cell growth and homeostasis is an additional contributor to the pathogenesis of AML (Dash and Gilliland, 2001).

The Ras/Raf/MAPK and PI3K/Akt/mTOR signaling pathways are two vital cascades that are physiologically relevant to diverse cell stimuli involved in differentiation, proliferation and apoptosis (Hanada et al., 2004; Lewis et al., 1998). Activation of these pathways has been associated with most AML cases (Martelli et al., 2006; Milella et al., 2001). One another common molecular defect, FLT3 mutation, is highly expressed in AML, accounting for 70-100% of all cases (Gilliland and Griffin, 2002). Specifically, the presence of ITDs in the juxtamembrane domain of FLT3 was found in nearly one third of patients with AML and is associated with a poor prognosis (Meshinchi et al., 2001). Therefore, these signal transduction cascades may represent promising areas to exploit with therapeutic intent in AML.

Interestingly, the aforementioned cascades consequently converge on the Mnk/eIF4E axis that plays a significant regulatory role in mRNA translation and malignant transformation. The phosphorylation of eIF4E by Mnk at Ser209 has been implicated in tumorigenesis and development (Furic et al., 2010; Waskiewicz et al., 1997). While Mnk activity is not essential

for normal cell growth (Ueda et al., 2004), the oncogenic activity of Mnk-driven eIF4E has shown to be vital for the proliferation and survival of cancer cells (Topisirovic et al., 2004; Wendel et al., 2007). Therefore, therapeutic targeting of the Mnk offers an opportunity for the treatment of cancer.

Mnks belong to a serine/threonine kinases family, which were identified as unique interacting proteins for ERK and p38 kinases in the MAPK cascade (Roux and Blenis, 2004; Waskiewicz et al., 1997). Two Mnk human genes have identified, expressing Mnk1 and Mnk2 proteins which are ~72% identical in their amino acid sequence (Slentz-Kesler et al., 2000). Alternative splicing in the two Mnk genes further revealed the existence of four isoforms: *Mnk1a*, *Mnk1b*, *Mnk2a* and *Mnk2b* (Scheper et al., 2003; Waskiewicz et al., 1997). Bearing a nuclear localization signal and a polybasic sequence in the common basic N-terminal stretch; all four isoforms preferentially localize in the nucleus and phosphorylate eIF4E efficiently.

The difference between the four isoforms arises from the C-termini, in which only the a-isoforms have a MAPK-binding site for interaction with ERK or p38 kinases (Parra et al., 2005). Despite this, Mnk1a and Mnk2a differ in basal activity as shown in *in vitro* studies (Scheper et al., 2001). Activation of ERK or p38 kinase could result in marked increase in the activation of the low basal activity of Mnk1a but negligibly influence the high basal activity of Mnk2a. Both Mnk1a and Mnk2a bind preferentially to ERK but only Mnk1a is a substrate for p38. In appreciation of the dissimilarity in the regulatory features of Mnk1 and Mnk2, these findings may indicate differences in activity and regulation of Mnks towards eIF4G to phosphorylate eIF4E.

An increasing body of evidence has demonstrated the potential anti-leukemic properties of pharmacologic Mnk inhibitors (Altman et al., 2013; Diab et al., 2014b; Lim et al., 2013).

Cercosporamide, a non-selective Mnk inhibitor (Konicek et al., 2011), reduces leukemic cell proliferation in MM6, K562 and U937 cell lines in a dose-dependent manner (Altman et al., 2013). The antitumor efficacy of cercosporamide in MV4-11 xenografts supports its Mnk-targeted anti-leukemic effects. The cell-specific effect, predominantly in leukemia cells, of Mnk inhibition, have been recently confirmed by our recent discovery of 5-(2-(phenylamino)pyrimidin-4-yl)thiazole-2(3*H*)-one Mnk inhibitors (Diab et al., 2014b).

We have recently identified thieno[2,3-*d*]pyrimidine derivatives as highly potent and selective Mnk inhibitors. Herein, a potent dual-specific Mnk1/2 inhibitor MNKI-19 and a selective Mnk2 inhibitor MNKI-85 were utilized to provide mechanistic insights into the effects of Mnk isoforms on leukemia cells. Both MNKI-19 and MNK-85 are able to reduce the level of phosphorylated eIF4E and subsequently cause G₁ phase cell cycle arrest and apoptosis in FLT3-ITD-expressed AML cells. The current report also demonstrates that a combined inhibition of Mnk1 and Mnk2 results in more pronounced cellular responses than targeting Mnk2 alone, supporting the Mnk inhibitors can be developed as potential anti-cancer agents.

Materials and Methods

Inhibitor compounds and proteins

Syntheses of MNKI-19 and MNKI-85 were described below. The Mnk inhibitor *N*³-(4-fluorophenyl)-1*H*-pyrazolo-[3,4-*d*]pyrimidine-3,4-diamine (CGP57380) was purchased from Sigma Aldrich, and used as a positive control. All compounds used were dissolved in dimethylsulfoxide (DMSO) at a stock concentration of 10 mM, and stored at -20 °C in small aliquots. eIF4E-derived peptides, TAMRA-DTATKSGSTTKNR, TAMRA-

DTATKSG(phospho)STTKNR and DTATKSGSTTKNR, were custom synthesized by Mimotopes Pty. Ltd. (Melbourne, Australia). Proteins Mnk1 and Mnk2 were purchased from Life Technologies and Merck Millipore, respectively.

Synthesis of MNKI-19 and MNKI-85

^1H and ^{13}C NMR spectra were recorded at 298 K on a Bruker AVANCE III HD 500 spectrometer (^1H at 500.16 MHz and ^{13}C at 125.76 MHz; Faellanden, Switzerland), and were analyzed using Bruker Topspin 3.2 software. ^1H and ^{13}C NMR spectra are referenced to ^1H signals of residual nondeuterated solvents and ^{13}C signals of deuterated solvents, respectively. ^1H NMR signals are reported with chemical shift values δ (ppm), multiplicity (s = singlet, d = doublet, t = triplet, q = quartet, dd = doublet of doublets, m = multiplet and br = broad), relative integral, coupling constants J (Hz) and assignments. High resolution mass spectra were recorded on an AB SCIEX TripleTOF 5600 mass spectrometer (Concord, ON, Canada), and ionization of all samples was carried out using ESI. Melting points were determined using an open capillary on a Stuart SMP10 melting point apparatus and are uncorrected. The purity of compounds used for biological evaluation was determined by analytic RP-HPLC which was carried out on a Shimadzu Prominence UFLC system (UltraFast Liquid Chromatograph, Kyoto, Japan) equipped with a CBM-20A communications bus module, a DGU-20A5R degassing unit, an LC-20AD liquid chromatograph pump, an SIL-20AHT auto-sampler, an SPD-M20A photo diode array detector, a CTO-20A column oven and a Phenomenex Kinetex 5u C18 100A 250 mm \times 4.60 mm column. Method A (gradient 5% to 95% CH_3OH containing 0.1% formic acid (FA) over 7 min at a flow rate of 1 mL/min, followed by 95% CH_3OH containing 0.1% FA over 13 min) and method B (gradient 5% to 95% CH_3CN containing 0.1% FA over 7 min at a flow rate of 1 mL/min, followed by 95%

CH₃CN containing 0.1% FA over 13 min) were used for analytic RP-HPLC. Data acquired from analytic RP-HPLC were processed using LabSolutions analysis software.

To a solution of methyl 4-((4-fluoro-2-isopropoxyphenyl)amino)-5-methylthieno[2,3-*d*]pyrimidine-6-carboxylate (200 mg, 0.533 mmol) in a mixture of THF/MeOH/H₂O (1:1:1, 60 mL) was added LiOH (382 mg, 16.0 mmol). The reaction mixture was stirred at room temperature overnight and washed with DCM (20 mL). The aqueous layer was heated at 50 °C for 10 min and acidified to pH 3 with 2 M HCl. The precipitate was filtered, washed with H₂O (3 × 25 mL) and dried under reduced pressure to give 4-((4-fluoro-2-isopropoxyphenyl)amino)-5-methylthieno[2,3-*d*]pyrimidine-6-carboxylic acid (MNKI-19) as a white solid (128 mg, 67%). *R*_F(DCM:MeOH = 9:1) 0.28. m.p. > 300 °C. ¹H NMR (DMSO-*d*₆): δ 1.32 (d, 6H, *J* 6.0, OCH(CH₃)₂), 3.07 (s, 3H, thiophene-CH₃), 4.75-4.80 (m, 1H, OCH(CH₃)₂), 6.80 (td, 1H, *J* 8.5 & 2.5, benzene-H), 7.07 (dd, 1H, *J* 11.0 & 2.5, benzene-H), 8.47 (s, 1H, NH), 8.54 (s, 1H, pyrimidine-H), 8.56 (dd, 1H, *J* 9.0 & 6.5, benzene-H) (one carboxylic acid proton signal not observed). ¹³C NMR (DMSO-*d*₆): δ 15.3, 21.7, 71.5, 101.1 (d, *J*_{C-F} 26.8), 106.1 (d, *J*_{C-F} 21.6), 117.8, 121.9 (d, *J*_{C-F} 9.4), 123.9, 125.0 (d, *J*_{C-F} 2.6), 137.5, 148.3 (d, *J*_{C-F} 10.6), 155.1, 156.1, 158.6 (d, *J*_{C-F} 239.0), 163.9, 166.3 (one carbon signal overlapping or obscured). HRMS (ESI) *m/z* 362.1500 [M+H]⁺; calcd. for C₁₇H₁₇FN₃O₃S⁺ 362.0969 [M+H]⁺. Anal. RP-HPLC Method A: *t*_R 16.95 min, purity > 97%; Method B: *t*_R 12.48 min, purity > 97%.

To a solution of 4-((4-fluoro-2-isopropoxyphenyl)amino)-5-methylthieno[2,3-*d*]pyrimidine-6-carboxylic acid (200 mg, 0.533 mmol) in DMF (3 mL) were added DIPEA (193 μL, 1.11 mmol) and HATU (316 mg, 0.830 mmol). The reaction mixture was stirred on an ice bath for 30 min. 2-Methoxypropylamine (54.0 μL, 0.609 mmol) was added, and the reaction mixture was stirred at room temperature overnight and concentrated under reduced pressure. The residue was dissolved in DCM (20 mL), washed with saturated NaHCO₃ (3 ×

20 mL), 10% citric acid (3×20 mL), H₂O (3×20 mL) and brine (3×20 mL), and concentrated under reduced pressure. The residue was purified by Biotage® FlashMaster Personal⁺ flash chromatography (silica gel, DCM ramping to DCM:EtOAc = 4:1) to give 4-((4-fluoro-2-isopropoxyphenyl)amino)-N-(2-methoxyethyl)-5-methylthieno[2,3-*d*]pyrimidine-6-carboxamide (MNKI-85) as a white solid (118 mg, 51%). *R*_F (DCM:EtOAc = 7:3) 0.54. m.p. 186-187 °C. ¹H NMR (CDCl₃): δ 1.43 (d, 6H, *J* 6.0, OCH(CH₃)₂), 3.06 (s, 3H, thiophene-CH₃), 3.41 (s, 3H, OCH₃), 3.56-3.60 (m, 2H, CH₂CH₂O), 3.63-3.67 (m, 2H, CH₂CH₂O), 4.64-4.69 (m, 1H, OCH(CH₃)₂), 6.34 (br s, 1H, CONH), 6.69 (dd, 1H, *J* 10.0 & 3.0, benzene-H), 6.73 (td, 1H, *J* 8.5 & 2.5, benzene-H), 8.47 (br s, 1H, pyrimidine-NH-benzene), 8.61 (s, 1H, pyrimidine-H), 8.77 (dd, 1H, *J* 9.0 & 6.5, benzene-H). ¹³C NMR (CDCl₃): δ 16.1, 22.2, 40.1, 59.1, 70.3, 71.9, 100.5 (d, *J*_{C-F} 27.0), 106.8 (d, *J*_{C-F} 21.6), 118.3, 121.7 (d, *J*_{C-F} 9.0), 124.9, 127.3, 132.9, 147.7 (d, *J*_{C-F} 9.5), 154.2, 156.2, 159.1 (d, *J*_{C-F} 241.5), 162.9 (two carbon signals overlapping or obscured). HRMS (ESI) *m/z* 419.1394 [M+H]⁺; calcd. for C₂₀H₂₄FN₄O₃S⁺ 419.1548 [M+H]⁺. Anal. RP-HPLC Method A: *t*_R 16.01 min, purity > 96%; Method B: *t*_R 11.98 min, purity > 96%.

Cell Culture

All leukemia cell lines including HL-60, K562, MOLM-13, MV4-11, PL-21, THP-1 and U937 cells were kindly provided by Prof. Richard D'Andrea (University of South Australia, Australia) and were maintained in Roswell Park Memorial Institute (RPMI)-1640 with 10% fetal bovine serum (FBS). The normal lung fibroblast cell line, WI-38, was obtained from the cell bank at the Centre for Drug Discovery and Development, University of South Australia, and was maintained in minimum essential media (MEM) with 10% FBS, 2 mM L-glutamine

and 1% non-essential amino acid. All cell lines were cultured in a humidified 37 °C, 5% CO₂ incubator.

Kinase Assays

Inhibition of CDK2/cyclin A1, CDK9/cyclin T1, CDK4/cyclin D1, FLT3, Pim-1, B-Raf, MAPK1 (ERK2), MAPK2, PKB α (Akt1), PI3K (p110 β /p85 α), SAPK2 α (p38 α) and mTOR was measured by radiometric assays using the Millipore KinaseProfiler™ services with ATP concentrations within 15 μ M of apparent K_m (app) for each kinase. For CDK2/cyclin A1, CDK9/cyclin T1, CDK4/cyclin D1, FLT3 and Pim-1 kinases, the IC₅₀ values were calculated from 10-point dose-response curves and apparent inhibition constants (K_i) were calculated from the IC₅₀ values and appropriate ATP values using the Cheng and Prusoff equation (Cheng and Prusoff, 1973). For kinase panel screen, the kinase activities were reported as remaining activities that were calculated as percentage relative to the averages of multiply 0 and 100% controls, at a compound concentration of 5 μ M.

IMAP™ TR-FRET Progressive Binding System

Each compound (1 and 10 μ M in 0.5% DMSO) was added to the kinase reaction containing 1 \times IMAP reaction buffer with Tween-20 dithiothreitol, distilled H₂O, TAMRA-labeled eIF4E peptide substrate and Mnk kinase in a total assay volume of 20 μ L. The kinase reaction was initiated by addition of ATP, incubated at 30 °C for 90 min and stopped with 60 μ L progressive binding solution (30% binding buffer A, 70% binding buffer B, progressive binding reagent (1:600) and terbium (Tb)-donor (1:400)), followed by incubation in the dark at room temperature for 5 h. After the incubation, the plate was read in an EnVision multi-

label plate reader (PerkinElmer, Beaconsfield, Buckinghamshire, UK). Excitation wavelength for Tb-donor was set at 330 nm while emissions were measured at 545 nm (Tb emission) and 572 nm (TR-FRET emission) in a time-resolved manner with a delay of 200 μ s. Positive and negative controls were performed in 0.5 % DMSO in the presence and absence of Mnk kinases, respectively.

ADP-GloTM Kinase Assay

The ADP-GloTM assay kits were purchased from Promega (Madison, WI, USA). Serial dilution of compounds with a dilution factor of 1:3 was performed to give 8 concentrations ranging from 10 μ M to 4.5 nM with 0.5% DMSO. Each compound was added to the kinase reaction containing 1 \times kinase reaction buffer, 0.1 mg/mL bovine serum albumin, distilled H₂O, eIF4E peptide substrate and Mnk kinase in a total assay volume of 15 μ L. The kinase reaction was initiated by addition of ATP, incubated at 30 °C for 45 min and stopped with 15 μ L ADP GloTM reagent, followed by incubation in the dark at room temperature for 40 min. 30 μ L kinase detection reagent was added. The mixture was further incubated for 40 min before reading in an EnVision multi-label plate reader (PerkinElmer, Beaconsfield, Buckinghamshire, UK). Positive and negative controls were performed with 0.5 % DMSO in the presence and absence of Mnk kinases, respectively.

Cell Viability Assays

Resazurin (Sigma Aldrich, Castle Hill, NSW) and MTT (3-(4,5-dimethylthiazol-2-yl)-2,5-diphenyltetrazolium bromide) (Life Technologies, Mulgrave, VIC) assays were performed on all leukemia cell lines and normal lung fibroblast, respectively, as previously reported (Diab

et al., 2014b). Compound concentrations required to inhibit 50% of cell growth (GI_{50}) were calculated using non-linear regression analysis.

Caspase-3/7 Assay

Activity of caspase-3/7 was measured using the Apo-ONE Homogeneous Caspase-3/7 kit (G7790 Promega, Madison, WI, USA) according to manufacturer instruction and analyzed using an EnVision multi-label plate reader (PerkinElmer, Beaconsfield, Buckinghamshire, UK).

Cell Cycle and Detection of Apoptosis

MOLM-13 and MV4-11 (1×10^5) cells were seeded and incubated overnight at 37 °C, 5% CO₂. Cells were centrifuged at $300 \times g$ for 5 min upon treatment with each compound. Cell pellets were collected and fixed with 70% ethanol on ice for 15 min, followed by centrifugation at $300 \times g$ for 5 min. The collected pellets were incubated with staining solution (50 µg/mL propidium iodide (PI), 0.1 mg/mL ribonuclease A, 0.05% Triton X-100) at 37 °C for an hour and analyzed with Gallios flow cytometer (Beckman Coulter, Brea, CA, USA). 1×10^5 of the remaining cells were used for the apoptotic assay with Annexin V-fluorescein isothiocyanate (FITC) Apoptosis Detection Kit (Becton Dickinson, Franklin Lakes, NJ, USA) following manufacturer's instructions. The samples were analyzed by fluorescence-activated cell sorting (FACS) with the flow cytometer within one hour of staining. Data were analyzed using Kaluza v1.2 (Beckman Coulter, Brea, CA, USA).

Western blots

Western blotting was performed as described previously (Wang et al., 2004). Antibodies used were as follows: Mnk2 and phosphorylated Rb at Thr821 (p-Rb^{T821}) (Abcam, Cambridge, England, UK), β -actin, caspase-3, CDK4, CDK6, cyclin D3, eIF4E, phosphorylated eIF4E at Ser209 (p-eIF4E^{S209}), 4E-BP1, phosphorylated 4E-BP1 at Thr37/46 (p-4E-BP1^{T37/46}) and Thr70 (p-4E-BP1^{T70}), phosphorylated p42/p44 at Thr202/Tyr204 (p-ERK^{T202/Y204}), Mcl-1, PARP, cleaved PARP, Mnk1, p38, phosphorylated p38 at Thr180/Tyr182 (p-p38^{T180/Y182}) (Cell Signaling Technologies), Bcl-2 (Dako, Kingsgrove, NSW), p-Rb^{T826} (Sigma Aldrich, Castle Hill, NSW) and p42/44 (Protein Simple). Both anti-mouse and anti-rabbit immunoglobulin G (IgG) horseradish peroxidase (HRP)-conjugated antibodies were obtained from Dako, Kingsgrove, NSW. Enhanced Chemiluminescence (ECL) reagents were obtained from GE Healthcare Life Sciences, Rydalmere, NSW.

Statistical Analyses

All experiments were performed in triplicate and repeated at least three times; representative experiments were selected for figures. Statistical significance of differences observed between experimental groups was determined using one-way analysis of variance (ANOVA), with a minimal level of significance at $p < 0.05$.

Results

MNKL-19 and MNKL-85 are potent and selective Mnk inhibitors

Thienopyrimidinyl derivative MNKI-19 inhibits Mnk1 and Mnk2 potently with K_i values of 0.186 and 0.068 μM , respectively, by biochemical assays (Table 1). MNKI-85 exhibits ~5-fold increased inhibitory activity against Mnk2 ($K_i = 0.031 \mu\text{M}$) when compared to MNKI-19, but is completely inactive against Mnk1. No inhibitory activities against CDK2A, CDK9T and CDK4D were detected with both compounds ($K_i > 10 \mu\text{M}$). To further profile kinase selectivity, MNKI-19 and MNKI-85 were tested against a panel of upstream activating kinases of Mnk, including B-Raf, MAPK1, MAPK2, Akt1, PI3K, p38 α and mTOR, at 5 μM (Figure 1). FLT3 protein is an upstream effector of both the Ras/Raf/MAPK and PI3K/Akt/mTOR pathways (Wander et al., 2014). As one of the downstream effectors of FLT3, Pim-1 was inhibited potently by cercosporamide (Konicek et al., 2011), it is thus of great interest to evaluate the inhibitory activities of the compounds against FLT3 and Pim-1. The results obtained from in-house IMAP assays for Mnk1 and Mnk2 at 1 μM of the tested compounds were included for comparison. Both compounds are inactive against most of the upstream kinases, with the exception that MNKI-19 displays moderate activity against Pim-1 ($K_i = 2.35 \mu\text{M}$, Table 1). However, it is 12- and 35-fold less active when compared to these of Mnk1 and Mnk2, respectively. Collectively, these data suggest the high specificity of MNKI-19 and MNKI-85 for Mnk.

MNKI-19 and MNKI-85 exhibit anti-leukemic activity

The anti-proliferative activity of both MNKI-19 and MNKI-85 were assessed on a panel of six AML cell lines and one CML cell line (Table 2) using 72 h resazurin assays. CGP57380 was included as a control. All compounds exhibited the greatest anti-proliferative effects on MOLM-13 and MV4-11, both of which expressed FLT3-ITD (Quentmeier et al., 2003), with GI_{50} values ranging between 5.65 and 8.81 μM . In contrast, at least 4-fold higher concentrations of compounds MNKI-19 and MNKI-85 were required to suppress the

proliferation of HL-60, K562, THP-1 and U937 (wild-type FLT3 expression). Surprisingly, PL-21 cells, expressing both wild-type (WT) and mutated alleles, showed less sensitivity in response to the same treatments. Different anti-proliferative effects on these cells have also been observed with CGP57380, which modestly suppressed cell proliferation with GI_{50} values ranging from 6.89 to 38.97 μ M, suggesting an alternative mechanism underlying the growth inhibitory effects for CGP57380. Taken together, these data suggest that cellular effects of the Mnk inhibitors are more pronounced against AML cells with FLT3-ITD expression than the non-mutated FLT3 cells.

It is worth noting that these thienopyrimidinyl derivatives also display cell-specific effect between cancerous and normal cells. The normal lung fibroblast WI-38 cells were insensitive to both MNKI-19 and MNKI-85 with GI_{50} values being 98.63 and 43.40 μ M, respectively (Table 2).

MNKI-19 and MNKI-85 inhibits the phosphorylation of eIF4E and 4E-BP1

We next examined cellular Mnk inhibition of MNKI-19 and MNKI-85 by Western blot analysis (Figure 2). MOLM-13 cells were treated with CGP57380, MNKI-19 or MNKI-85 at 5 μ M and/or 10 μ M and 20 μ M for a period of 1 h. As shown in Figure 2A, both MNKI-19 and MNK-85 completely depleted the phosphorylation of eIF4E at Ser209 (p-eIF4E^{S209}) at a lower concentration (*i.e.* 5 μ M) whereas CGP57380 moderately suppressed p-eIF4E^{S209} within the same concentration. These results confirm the cellular inhibition of Mnk and the relative potency of MNKI-19 and MNKI-85 against Mnks over CGP57380. The treatment caused no changes in the expressions of total eIF4E, Mnk1 and Mnk2 proteins. To assess the Mnk-targeting specificity, the effects of MNKI-19 or MNKI-85 on the upstream activating kinases, including p38 MAPK, ERK, eIF4E-binding protein 1 (4E-BP1) and their phosphorylated forms, were analyzed in MOLM-13 cells. Incubation with MNKI-19 for 1 h

has up-regulated an early transient phosphorylation of ERK and p38 in a dose-dependent manner, without affecting their total levels. The expression levels of protein 4E-BP1 and its phosphorylated forms at Thr37/46 and Thr70 are not affected, which is consistent to the kinase assays showing no inhibitory activity against mTOR with MNKI-19 and MNKI-85 (Figure 1). Similar effects were seen in CGP57380-treated cells but not in MNKI-85. However, little to no effect on the levels of p38 and ERK proteins and their phosphorylated forms was observed after treating MOLM-13 with 20 μ M compounds for 24 h (Figure 2B).

At 24 h, the complete abolition of p-eIF4E^{S209} by Mnk inhibitors gave rise to a reduction in the phosphorylation of 4E-BP1 at Thr37/46 (Figure 2C and Supplemental Figure 1) and Thr70 (Figure 2C), particularly at the latter in a dose-dependent manner, in MOLM-13 cells.

MNKI-19 and MNKI-85 arrest cancer cells in the G₁ phase of cell cycle *via* down-regulating CDK4 and cyclin D3

We next investigated whether the anti-proliferative activity of MNKI-19 and MNKI-85 was a consequence of cell cycle effects. As shown in Figure 3A, treatment of MOLM-13 cells with MNKI-19 or MNKI-85 at 5 μ M for 24 h resulted in the accumulation of G₁ cells, which was accompanied by a loss in cell population at the G₂/M phase. This is consistent with previous studies (Diab et al., 2014b; Zhang et al., 2008). The cell cycle effect of MNKI-19 was found to behave in a dose- and time-dependent manner. Consistently, this was observed with MV4-11 cells after treatment with the compounds (Figure 3B). However, in the case of MNKI-85, there was no significant change in the cell cycle distribution observed with longer treatment time. Time-course Western blot analysis was conducted to study the levels of key proteins involved in cell cycle after treatment of MOLM-13 cells with compound inhibitors for 1 h and 24 h. Attempts were made to study the expression level of cyclin D1 in MOLM-13 cells but the protein was too weak to be detected (data not shown), hence cyclin D3 was

pursued. In human somatic cells, the G₁ to S phase transition is tightly regulated by the cyclin-D/CDK4/6 proteins, along with their downstream target, retinoblastoma (Rb) protein (Neganova and Lako, 2008). As shown in Figure 3C, no significant changes were detected in these cell cycle regulators at the early time-point (*i.e.* 1 h) (see also Supplemental Figure 2). However, 24 h incubation of MOLM-13 cells with Mnk inhibitors resulted in the suppression of cyclin D3 expression in a dose-dependent manner (Figure 3D). CDK4 was also down-regulated by Mnk inhibitors at low concentration.

To investigate whether the perturbation of cell cycle progression is a consequence of CDK4 activity, the phosphorylation of Rb at both CDK4-specific Thr826 (p-Rb^{T826}) site (Macdonald and Dick, 2012) was also measured. A decreased level of p-Rb^{T826} was detected upon treatment of MOLM-13 cells with 20 μ M of MNKI-19 or MNKI-85 (Figure 3D, Supplemental Figure 3), indicating the loss of CDK4 activity and restricting the G₁ to S transition. This observation is further supported by kinase assays showing that both MNKI-19 and MNKI-85 have no inhibitory effect on CDK4 kinase activity (Table 1), implying the decreased CDK4 protein expression is a consequence of the down-regulating Mnk/eIF4E-mediated protein synthesis of cyclin D3. In contrast, little effect on CDK6 or CDK6-specific p-Rb^{T821} levels was observed (Figure 3E, Supplemental Figure 4), supporting the relative importance of CDK4 over CDK6 in the cell cycle progression (Neganova and Lako, 2008).

MNKI-19 and MNKI-85 induce apoptosis in FLT3-ITD-expressed AML cells

The apoptotic mechanism of action by Mnk inhibitors was further examined using annexin V/propidium iodide (PI) staining. Exposure of MOLM-13 or MV4-11 cells to either MNKI-19, MNKI-85 or CGP57380 at a concentration of 10 or 20 μ M for 24 h caused 2-4-fold increase in apoptotic cells (annexin V+/PI- and annexin V+/PI+) when compared to untreated cells (Figure 4A-B). Consistent with the cell cycle profile, MNKI-19 induced significant

apoptosis in a dose- and time-dependent manner. While the proteins involved in the apoptosis mechanism, including Mcl-1, Bcl-2, PARP and caspase-3, were not affected in MOLM-13 cells at the early time-point (*i.e.* 1 h) (Figure 4C), Western blot analysis revealed the down-regulation of the anti-apoptotic protein Mcl-1 and/or an increase of PARP cleavage after exposure to 5 μ M of MNKI-19, MNKI-85 or CGP57380 for 24 h (Figure 4D), indicating the apoptotic effect caused by the inhibition of Mnks. The levels of Bcl-2 remain unchanged (Figure 4E), which is in agreement with our previous results obtained using MV4-11 (Diab et al., 2014b).

In conjunction with no aberration in full length caspase-3 protein levels (Figure 4E) and no detectable caspase-3/7 activity (Figure 4F), the data indicate that Mnk inhibitor-induced apoptosis in MOLM-13 and MV4-11 cells may be independent of caspases-3 and -7.

Discussion

Screening against a panel of 7 leukemia cell lines with various FLT3 mutational statuses revealed the selective Mnk inhibitors MNKI-19 and MNKI-85 are particularly effective in suppressing the growth of FLT3/ITD-expressing AML cells, including MOLM-13 and MV4-11. PL-21 cells, in contrast, expressing both WT and mutated alleles (Quentmeier et al., 2003), were less sensitive to these compounds. However, it remains debatable that PL-21 cells could only express the WT allele (Yokota et al., 1997). Nevertheless, the differences in the sensitivity between the cell lines could be attributed to the different subtypes, which are classified based on the morphology and immunohistochemistry of myeloid neoplasms (Bennett et al., 1985). Both MOLM-13 and MV4-11 are acute monoblastic leukemia cells (M5/M5a) (Quentmeier et al., 2003) that carry the respective t(9,11) and t(4,11) chromosomal translocations, resulting in the fusion proteins MLL-AF9 and MLL-AF4, respectively

(Andersson et al., 2005; Matsuo et al., 1997). Of note, these subtypes of AML are correlated with aberrant up-regulation of eIF4E (Topisirovic et al., 2003), which is absent in the less mature promyelocytic cells (M3; PL-21 cells) (Quentmeier et al., 2003). As a comparator, THP-1 cells with the t(9,11) chromosomal translocation and no detectable FLT3-ITD expression, exhibited negligible sensitivity to MNKI-19 and MNKI-85 (> 12-fold). Similarly, HL-60, U937 and K562, which do not express ITD mutations, have no cytotoxic effects when treated with the compounds for up to 3 days. These results are in agreement with a previous study, in which inhibiting 50% of cell growth in K562, U937 and MM6 cell lines after 5-day treatment also required > 10 μ M of cercosporamide (Altman et al., 2013). CGP57380, on the other hand, is not particularly selective against the ITD-positive cells, indicating an alternative mechanism underlying the growth inhibitory effects. When considered together, concurrently activated upstream signaling pathways of Mnks with overexpressed eIF4E levels as characterized by the combined FLT3-ITD mutations and M5 subtypes, may serve as the right platform for investigation of the anti-leukemic effects of Mnk-specific inhibitors.

Western blot analysis further confirmed the role of MNKI-19 and MNKI-85 as potent Mnk inhibitors, as evidenced by the blockage of eIF4E^{S209} phosphorylation. As Mnks are important convergence nodes of the MAPK pathways (Chappell et al., 2011; Faivre et al., 2006), the expression of the upstream effectors, p38 and ERK, was also investigated. Interestingly, an early transient phosphorylation of ERK and p38 was found to be up-regulated upon incubation with MNKI-19 for 1 h, without affecting their total levels. Similar effects were seen in CGP57380-treated cells but not in MNKI-85. This could be attributed to the induction of negative-feedback mechanism upon Mnk1 inhibition as both ERK and p38 are substrates for Mnk1 (Waskiewicz et al., 1997). Such an observation is consistent to a study done by Zhang *et al.* who has reported that CGP57380-mediated ERK and Mnk activation was determined at early time-point (*i.e.* 30 min) and followed by a second late

phosphorylation starting at 24 h in the Bcr-Abl-dependent cells (Zhang et al., 2008). Little to no effect on the levels of ERK and p38 proteins and their phosphorylated forms was observed after treating MOLM-13 with 20 μ M compounds for 24 h, supporting that the sustained phosphorylation at late time-point is dependent on the presence of Bcr-Abl and signifying the specific effect of our Mnk inhibitors on Mnk/eIF4E. The compounds were also evaluated against a panel of upstream activating kinases, including B-Raf, ERK, p38 α , PI3K, Akt1 and mTOR, using biochemical assays, and showed no significant kinase inhibitory activity, supporting selectivity of the compounds.

Interestingly, down-regulations of the levels of phosphorylated 4E-BP1 at Thr37/46 and Thr70 (the two most priming phosphorylation events for the upstream effector mTOR) (Gingras et al., 2001) were detected in MOLM-13 cells treated with either MNKI-19 or MNKI-85. Binding of eIF4E to 4E-BP1 is regulated by hierarchical multisite phosphorylation and the role of the phosphorylation site at Thr37/46 on eIF4E binding remains controversial: several studies claimed that the phosphorylation of Thr37/46 has little effect on the binding of eIF4E (Gingras et al., 1999; Karim et al., 2001), while the other group showed that a significant reduction in eIF4E-binding affinity was induced by such a phosphorylation event (Burnett et al., 1998). However, mutations of these residues and/or Thr70 to alanine, have significantly led to the dissociation of eIF4E from 4E-BP1 (Gingras et al., 2001), confirming the important role of these phosphorylation sites on the eIF4E/4E-BP1 equilibrium.

In light of these findings, it is speculated that a negative-feedback regulatory mechanism involving the equilibrium shift towards the eIF4E/4E-BP1 complex could be triggered in the compound-treated cells. Translation processes involve the assembly of several eIF4 translational factors, including the eIF4E and activated Mnks to form the eIF4F complex (Hou et al., 2012). Inhibition of Mnks, especially Mnk2, may increase the levels of eIF4E in the cells as the formation of eIF4F complex has been disrupted. As the Akt/mTOR pathway is

overly activated in FLT3-ITD MOLM-13 cells (Hayakawa et al., 2000), it is suspected that the up-regulated eIF4E levels have initiated the negative-feedback mechanism of Akt/mTOR to dephosphorylate 4E-BP1. Upon hypo-phosphorylation, 4E-BP1 interacts strongly with eIF4E (Khaleghpour et al., 1999). While our compounds were inactive to the upstream kinases in the Akt/mTOR pathway, particularly mTOR, it is believed that the dephosphorylation events were induced upon Mnk inhibition.

Complementary to this, a recent study used CGP57380 to investigate the effect of eIF4E phosphorylation on translation initiation, showing that the amount of eIF4G in the eIF4F complex was decreased when treated with the compound (Li et al., 2010). This implies that inhibiting Mnks may reduce the eIF4F assembly. Another recent study also suggested that the dissociation of 4E-BP1 is highly dependent on the Mnk1-mediated eIF4E phosphorylation (Das et al., 2013). The dephosphorylation of 4E-BP1 by MNKI-19 could be also due to the Pim-1 inhibition as shown in the kinase assay. The 4E-BP1 has recently been identified as a target of Pim-1 in the FLT3-ITD-driven activation of STAT-5. Pim-1 inhibitors have significantly reduced the p-4E-BP1^{T37/46} in the FLT3-ITD AML cells (Chen et al., 2011). However, more studies on the binding affinity of compounds MNKI-19 and MNKI-85 for the relevant proteins, such as eIF4G and 4E-BP1, are required to unveil the underlying mechanism.

The oncogenic role of eIF4E has been reported in the cell cycle progression (Diab et al., 2014a). D-type cyclins, as G₁ progression factors, play a vital role in enhancing the G₁ to S transition through binding to the CDK4/6 (Sherr, 1995). Elevated eIF4E levels have been shown to enhance the translational levels of a wide array of malignancy-related mRNAs involved in the regulation of cell senescence, proliferation and apoptosis, including cyclin D1 and Mcl-1 (Zimmer et al., 2000), whereas the oncogenic functions of eIF4E are closely linked to its phosphorylation by Mnks (Diab et al., 2014a; Ueda et al., 2010). Consistent with

previous studies (Diab et al., 2014b; Teo et al., 2015; Zhang et al., 2008), Mnk inhibitors in the current study triggered a cell cycle arrest in both MOLM-13 and MV4-11 cells by disrupting the transition of G₁ to S phase. Such an effect is likely to be the result of decreased expression of the key cell cycle regulators, including CDK4 and cyclin D3, which further hampered the phosphorylation of Rb at the CDK4-specific Thr826 site (Macdonald and Dick, 2012). This is further supported when kinase assays showed both MNKI-19 and MNKI-85 have no effect on CDK4 kinase activity ($K_i > 10 \mu\text{M}$). Previous studies also demonstrated the importance of cyclin D3 at the translational level over other D-type cyclins (Prabhu et al., 2007; Zhang et al., 2008).

Collectively, these results indicate that the effect of eIF4E-mediated cell cycle arrest is through phosphorylation by Mnks. While MNKI-19 increased the G₁ cell accumulation in a time-dependent manner, MNKI-85 failed to show the similar cell cycle effect (Figure 3A and B), suggesting that targeting a combination of Mnk1 and Mnk2 may be more effective than one of the isoforms alone in preventing cell cycle progression. Our observation agrees with a recent study of a series of Mnk degrading agents which showed to induce a G₁/G₀ cell cycle arrest, along with the down-regulation of cyclin D3 and CDK4 in MDA-MB-231 cells (Ramalingam et al., 2014).

The apoptotic effect of Mnk inhibitors is likely mediated through the 4E-BP1/eIF4E axis. Several lines of evidence have indicated the positive correlation between the suppression of eIF4E by binding to 4E-BP1 and induction of apoptosis (Clemens, 2001; Yellen et al., 2013). To date, Mnk1 and Mnk2 are the only identified kinases that phosphorylate eIF4E, and phosphorylation of eIF4E modulates cap-dependent translation. In addition, eIF4E phosphorylation can be down-regulated by 4E-BP1 binding (Li et al., 2010), this has, hence, raised the possibility that inhibiting Mnks triggers the dephosphorylation of 4E-BP1 and results in the reduction of cap-dependent protein synthesis, including Mcl-1. In contrast, the

significant induction of G₁ arrest and apoptosis by MNKI-19 could also be an additive effect of Pim-1 inhibition. Previous study has shown that Pim-1 inhibitors reduced Mcl-1 and induced apoptosis in FLT3-ITD AML cells (Chen et al., 2011).

We have shown that inhibition of eIF4E phosphorylation with Mnk inhibitors is associated with an increase in cell death. An increase cleavage of PARP and a marked suppression of Mcl-1 levels were observed. Lack of procaspase-3 processing and caspase-3/7 activation suggest that the apoptotic cell death by Mnk inhibitors may be *via* a caspase-independent mechanism. In contrast, a recent study demonstrated a caspase-dependent apoptosis was induced with Mnk degrading agents in breast cancer cell lines (Ramalingam et al., 2014). Perhaps, modes of action are contingent on compounds treated and cell lines tested. However, it is noteworthy that a combined use of Mnk1 and Mnk2, as represented by MNKI-19, gives rise to a more pronounced apoptosis than inhibiting Mnk2 alone (MNKI-85).

Acknowledgements

We are grateful to Professor Richard D'Andrea (University of South Australia) for the generous supply of the AML cell lines.

Authorship Contributions

Research design: Wang and Teo.

Conducted experiments: Teo and Basnet.

Contributed new reagents or analytical tools: Yang and Yu.

Performed data analysis: Teo, Lam, Basnet, Albrecht and Wang.

Wrote or contributed to the writing of the manuscript: Teo, Wang, Yu and Sykes.

References

Altman JK, Szilard A, Konicek BW, Iversen PW, Kroczyńska B, Glaser H, Sassano A, Vakana E, Graff JR and Platanias LC (2013) Inhibition of Mnk kinase activity by cercosporamide and suppressive effects on acute myeloid leukemia precursors. *Blood* **121**: 3675-3681.

Andersson A, Eden P, Lindgren D, Nilsson J, Lassen C, Heldrup J, Fontes M, Borg A, Mitelman F, Johansson B, Hoglund M and Fioretos T (2005) Gene expression profiling of leukemic cell lines reveals conserved molecular signatures among subtypes with specific genetic aberrations. *Leukemia* **19**: 1042-1050.

Bennett JM, Catovsky D, Daniel MT, Flandrin G, Galton DA, Gralnick HR and Sultan C (1985) Proposed revised criteria for the classification of acute myeloid leukemia. A report of the French-American-British Cooperative Group. *Ann Intern Med* **103**: 620-625.

Burnett PE, Barrow RK, Cohen NA, Snyder SH and Sabatini DM (1998) RAFT1 phosphorylation of the translational regulators p70 S6 kinase and 4E-BP1. *Proc Natl Acad Sci USA* **95**: 1432-1437.

Chappell WH, Steelman LS, Long JM, Kempf RC, Abrams SL, Franklin RA, Basecke J, Stivala F, Donia M, Fagone P, Malaponte G, Mazzarino MC, Nicoletti F, Libra M, Maksimovic-Ivanic D, Mijatovic S, Montalto G, Cervello M, Laidler P, Milella M, Tafuri A, Bonati A, Evangelisti C, Cocco L, Martelli AM and McCubrey JA (2011)

Ras/Raf/MEK/ERK and PI3K/PTEN/Akt/mTOR inhibitors: rationale and importance to inhibiting these pathways in human health. *Oncotarget* **2**: 135-164.

Chen LS, Redkar S, Taverna P, Cortes JE and Gandhi V (2011) Mechanisms of cytotoxicity to Pim kinase inhibitor, SGI-1776, in acute myeloid leukemia. *Blood* **118**: 693-702.

Cheng Y and Prusoff WH (1973) Relationship between the inhibition constant (K₁) and the concentration of inhibitor which causes 50 per cent inhibition (I₅₀) of an enzymatic reaction. *Biochem Pharmacol* **22**: 3099-3108.

Clemens MJ (2001) Translational regulation in cell stress and apoptosis. Roles of the eIF4E binding proteins. *J Cell Mol Med* **5**: 221-239.

Das F, Ghosh-Choudhury N, Bera A, Kasinath BS and Choudhury GG (2013) TGFβ-induced PI 3 kinase-dependent Mnk-1 activation is necessary for Ser-209 phosphorylation of eIF4E and mesangial cell hypertrophy. *J Cell Physiol* **228**: 1617-1626.

Dash A and Gilliland DG (2001) Molecular genetics of acute myeloid leukaemia. *Best Pract Res Clin Haematol* **14**: 49-64.

Diab S, Kumarasiri M, Yu M, Teo T, Proud C, Milne R and Wang S (2014a) MAP kinase-interacting kinases-emerging targets against cancer. *Chem Biol* **21**: 441-452.

Diab S, Teo T, Kumarasiri M, Li P, Yu M, Lam F, Basnet SK, Sykes MJ, Albrecht H, Milne R and Wang S (2014b) Discovery of 5-(2-(phenylamino)pyrimidin-4-yl)thiazol-2(3H)-one

derivatives as potent Mnk2 inhibitors: synthesis, SAR analysis and biological evaluation. *ChemMedChem* **9**: 962-972.

Faivre S, Djelloul S and Raymond E (2006) New paradigms in anticancer therapy: targeting multiple signaling pathways with kinase inhibitors. *Semin Oncol* **33**: 407-420.

Furic L, Rong L, Larsson O, Koumakpayi IH, Yoshida K, Brueschke A, Petroulakis E, Robichaud N, Pollak M and Gaboury LA (2010) eIF4E phosphorylation promotes tumorigenesis and is associated with prostate cancer progression. *Proc Natl Acad Sci USA* **107**: 14134-14139.

Gilliland DG and Griffin JD (2002) Role of FLT3 in leukemia. *Curr Opin Hematol* **9**: 274-281.

Gilliland DG, Jordan CT and Felix CA (2004) The molecular basis of leukemia. *Hematology Am Soc Hematol Educ Program* **2004**: 80-97.

Gingras AC, Gygi SP, Raught B, Polakiewicz RD, Abraham RT, Hoekstra MF, Aebersold R and Sonenberg N (1999) Regulation of 4E-BP1 phosphorylation: a novel two-step mechanism. *Genes Dev* **13**: 1422-1437.

Gingras AC, Raught B, Gygi SP, Niedzwiecka A, Miron M, Burley SK, Polakiewicz RD, Wyslouch-Cieszyńska A, Aebersold R and Sonenberg N (2001) Hierarchical phosphorylation of the translation inhibitor 4E-BP1. *Genes Dev* **15**: 2852-2864.

Hanada M, Feng J and Hemmings BA (2004) Structure, regulation and function of PKB/AKT--a major therapeutic target. *Biochim Biophys Acta* **1697**: 3-16.

Hayakawa F, Towatari M, Kiyoi H, Tanimoto M, Kitamura T, Saito H and Naoe T (2000) Tandem-duplicated Flt3 constitutively activates STAT5 and MAP kinase and introduces autonomous cell growth in IL-3-dependent cell lines. *Oncogene* **19**: 624-631.

He LZ, Tribioli C, Rivi R, Peruzzi D, Pelicci PG, Soares V, Cattoretti G and Pandolfi PP (1997) Acute leukemia with promyelocytic features in PML/RARalpha transgenic mice. *Proc Natl Acad Sci USA* **94**: 5302-5307.

Hou J, Lam F, Proud C and Wang S (2012) Targeting Mnk1 for cancer therapy. *Oncotarget* **3**: 118-131.

Karim MM, Hughes JM, Warwicker J, Scheper GC, Proud CG and McCarthy JE (2001) A quantitative molecular model for modulation of mammalian translation by the eIF4E-binding protein 1. *J Biol Chem* **276**: 20750-20757.

Khaleghpour K, Pyronnet S, Gingras AC and Sonenberg N (1999) Translational homeostasis: eukaryotic translation initiation factor 4E control of 4E-binding protein 1 and p70 S6 kinase activities. *Mol Cell Biol* **19**: 4302-4310.

Konicek BW, Stephens JR, McNulty AM, Robichaud N, Peery RB, Dumstorf CA, Dowless MS, Iversen PW, Parsons S, Ellis KE, McCann DJ, Pelletier J, Furic L, Yingling JM, Stancato LF, Sonenberg N and Graff JR (2011) Therapeutic inhibition of MAP kinase

interacting kinase blocks eukaryotic initiation factor 4E phosphorylation and suppresses outgrowth of experimental lung metastases. *Cancer Res* **71**: 1849-1857.

Lewis TS, Shapiro PS and Ahn NG (1998) Signal transduction through MAP kinase cascades. *Adv Cancer Res* **74**: 49-139.

Li Y, Yue P, Deng X, Ueda T, Fukunaga R, Khuri FR and Sun SY (2010) Protein phosphatase 2A negatively regulates eukaryotic initiation factor 4E phosphorylation and eIF4F assembly through direct dephosphorylation of Mnk and eIF4E. *Neoplasia* **12**: 848-855.

Lim S, Saw TY, Zhang M, Janes MR, Nacro K, Hill J, Lim AQ, Chang CT, Fruman DA, Rizzieri DA, Tan SY, Fan H, Chuah CT and Ong ST (2013) Targeting of the MNK-eIF4E axis in blast crisis chronic myeloid leukemia inhibits leukemia stem cell function. *Proc Natl Acad Sci USA* **110**: E2298-2307.

Macdonald JJ and Dick FA (2012) Posttranslational modifications of the retinoblastoma tumor suppressor protein as determinants of function. *Genes Cancer* **3**: 619-633.

Martelli AM, Nyakern M, Tabellini G, Bortul R, Tazzari PL, Evangelisti C and Cocco L (2006) Phosphoinositide 3-kinase/Akt signaling pathway and its therapeutic implications for human acute myeloid leukemia. *Leukemia* **20**: 911-928.

Matsuo Y, MacLeod RA, Uphoff CC, Drexler HG, Nishizaki C, Katayama Y, Kimura G, Fujii N, Omoto E, Harada M and Orita K (1997) Two acute monocytic leukemia (AML-M5a) cell lines (MOLM-13 and MOLM-14) with interclonal phenotypic heterogeneity showing

MLL-AF9 fusion resulting from an occult chromosome insertion, ins(11;9)(q23;p22p23).
Leukemia **11**: 1469-1477.

Meshinchi S, Woods WG, Stirewalt DL, Sweetser DA, Buckley JD, Tjoa TK, Bernstein ID and Radich JP (2001) Prevalence and prognostic significance of Flt3 internal tandem duplication in pediatric acute myeloid leukemia. *Blood* **97**: 89-94.

Milella M, Kornblau SM, Estrov Z, Carter BZ, Lapillonne H, Harris D, Konopleva M, Zhao S, Estey E and Andreeff M (2001) Therapeutic targeting of the MEK/MAPK signal transduction module in acute myeloid leukemia. *J Clin Invest* **108**: 851-859.

Neganova I and Lako M (2008) G1 to S phase cell cycle transition in somatic and embryonic stem cells. *J Anat* **213**: 30-44.

Parra JL, Buxade M and Proud CG (2005) Features of the catalytic domains and C termini of the MAPK signal-integrating kinases Mnk1 and Mnk2 determine their differing activities and regulatory properties. *J Biol Chem* **280**: 37623-37633.

Prabhu S, Saadat D, Zhang M, Halbur L, Fruehauf JP and Ong ST (2007) A novel mechanism for Bcr-Abl action: Bcr-Abl-mediated induction of the eIF4F translation initiation complex and mRNA translation. *Oncogene* **26**: 1188-1200.

Quentmeier H, Reinhardt J, Zaborski M and Drexler HG (2003) FLT3 mutations in acute myeloid leukemia cell lines. *Leukemia* **17**: 120-124.

Ramalingam S, Gediya L, Kwegyir-Afful AK, Ramamurthy VP, Purushottamachar P, Mbatia H and Njar VC (2014) First MNKs degrading agents block phosphorylation of eIF4E, induce apoptosis, inhibit cell growth, migration and invasion in triple negative and Her2-overexpressing breast cancer cell lines. *Oncotarget* **5**: 530-543.

Roux PP and Blenis J (2004) ERK and p38 MAPK-activated protein kinases: a family of protein kinases with diverse biological functions. *Microbiol Mol Biol Rev* **68**: 320-344.

Scheper GC, Morrice NA, Kleijn M and Proud CG (2001) The mitogen-activated protein kinase signal-integrating kinase Mnk2 is a eukaryotic initiation factor 4E kinase with high levels of basal activity in mammalian cells. *Mol Cell Biol* **21**: 743-754.

Scheper GC, Parra JL, Wilson M, Van Kollenburg B, Vertegaal AC, Han ZG and Proud CG (2003) The N and C termini of the splice variants of the human mitogen-activated protein kinase-interacting kinase Mnk2 determine activity and localization. *Mol Cell Biol* **23**: 5692-5705.

Sherr CJ (1995) D-type cyclins. *Trends Biochem Sci* **20**: 187-190.

Slentz-Kesler K, Moore JT, Lombard M, Zhang J, Hollingsworth R and Weiner MP (2000) Identification of the human Mnk2 gene (MKNK2) through protein interaction with estrogen receptor beta. *Genomics* **69**: 63-71.

Teo T, Yu M, Yang Y, Gillam T, Lam F, Sykes MJ and Wang S (2015) Pharmacologic co-inhibition of Mnks and mTORC1 synergistically suppresses proliferation and perturbs cell cycle progression in blast crisis-chronic myeloid leukemia cells. *Cancer Lett* **357**: 612-623.

Topisirovic I, Guzman ML, McConnell MJ, Licht JD, Culjkovic B, Neering SJ, Jordan CT and Borden KL (2003) Aberrant eukaryotic translation initiation factor 4E-dependent mRNA transport impedes hematopoietic differentiation and contributes to leukemogenesis. *Mol Cell Biol* **23**: 8992-9002.

Topisirovic I, Ruiz-Gutierrez M and Borden KL (2004) Phosphorylation of the eukaryotic translation initiation factor eIF4E contributes to its transformation and mRNA transport activities. *Cancer Res* **64**: 8639-8642.

Ueda T, Sasaki M, Elia AJ, Chio IIC, Hamada K, Fukunaga R and Mak TW (2010) Combined deficiency for MAP kinase-interacting kinase 1 and 2 (Mnk1 and Mnk2) delays tumor development. *Proc Natl Acad Sci USA* **107**: 13984-13990.

Ueda T, Watanabe-Fukunaga R, Fukuyama H, Nagata S and Fukunaga R (2004) Mnk2 and Mnk1 are essential for constitutive and inducible phosphorylation of eukaryotic initiation factor 4E but not for cell growth or development. *Mol Cell Biol* **24**: 6539-6549.

Wander SA, Levis MJ and Fathi AT (2014) The evolving role of FLT3 inhibitors in acute myeloid leukemia: quizartinib and beyond. *Ther Adv Hematol* **5**: 65-77.

Wang S, Wood G, Meades C, Griffiths G, Midgley C, McNae I, McInnes C, Anderson S, Jackson W, Mezna M, Yuill R, Walkinshaw M and Fischer PM (2004) Synthesis and biological activity of 2-anilino-4-(1H-pyrrol-3-yl) pyrimidine CDK inhibitors. *Bioorg Med Chem Lett* **14**: 4237-4240.

Waskiewicz AJ, Flynn A, Proud CG and Cooper JA (1997) Mitogen-activated protein kinases activate the serine/threonine kinases Mnk1 and Mnk2. *EMBO J* **16**: 1909-1920.

Wendel HG, Silva RLA, Malina A, Mills JR, Zhu H, Ueda T, Watanabe-Fukunaga R, Fukunaga R, Teruya-Feldstein J and Pelletier J (2007) Dissecting eIF4E action in tumorigenesis. *Genes Dev* **21**: 3232-3237.

Yellen P, Chatterjee A, Preda A and Foster DA (2013) Inhibition of S6 kinase suppresses the apoptotic effect of eIF4E ablation by inducing TGF-beta-dependent G1 cell cycle arrest. *Cancer Lett* **333**: 239-243.

Yokota S, Kiyoi H, Nakao M, Iwai T, Misawa S, Okuda T, Sonoda Y, Abe T, Kahsima K, Matsuo Y and Naoe T (1997) Internal tandem duplication of the FLT3 gene is preferentially seen in acute myeloid leukemia and myelodysplastic syndrome among various hematological malignancies. A study on a large series of patients and cell lines. *Leukemia* **11**: 1605-1609.

Yuan Y, Zhou L, Miyamoto T, Iwasaki H, Harakawa N, Hetherington CJ, Burel SA, Lagasse E, Weissman IL, Akashi K and Zhang DE (2001) AML1-ETO expression is directly involved in the development of acute myeloid leukemia in the presence of additional mutations. *Proc Natl Acad Sci USA* **98**: 10398-10403.

Zhang M, Fu W, Prabhu S, Moore JC, Ko J, Kim JW, Druker BJ, Trapp V, Fruehauf J and Gram H (2008) Inhibition of polysome assembly enhances imatinib activity against chronic myelogenous leukemia and overcomes imatinib resistance. *Mol Cell Biol* **28**: 6496-6509.

Zimmer SG, DeBenedetti A and Graff J (2000) Translational control of malignancy: the mRNA cap-binding protein, eIF-4E, as a central regulator of tumor formation, growth, invasion and metastasis. *Anticancer Res* **20**: 1343-1351.

Footnotes

This work was supported by the Australian Government National Health and Medical Research Council [Grant 1050825], and the Beat Cancer Project Principal Cancer Research Fellowship by South Australian Health and Medical Research Institute to S.W..

Legends for Figure

Figure 1. Selectivity of MNKI-19 and MNKI-85 against a panel of kinases. The remaining percentages of kinase activity upon treatment with each compound at 5 μ M concentration are shown, unless otherwise specified. Both Mnk1 and Mnk2 are tested by the in-house IMAF assays at 1 μ M of compound inhibitors. 15 μ M within K_m of ATP for each kinase is used in the assays. Data represent one repeat and kinases that show < 50% in kinase activity upon compounds treatment are further evaluated with dose-response analysis to obtain their apparent inhibition constants (K_i) as shown in Table 1.

Figure 2. Western blot analysis of key proteins involved in the Ras/Raf/MAPK and PI3K/Akt/mTOR pathways in MOLM-13 cells treated with CGP57380, MNKI-19 and MNKI-85 for (A) 1 h and (B-C) 24 h. In A and C, compounds are tested at 5 μ M and/or 10 μ M and 20 μ M whereas in B, compounds are used at 20 μ M. Antibodies used and the protein molecular weight marker are indicated on the left and right sides, respectively, of each panel. DMSO diluent is used as a control and β -actin is used as an internal loading control. A representative blot is selected from at least two independent repeats.

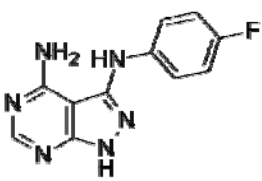

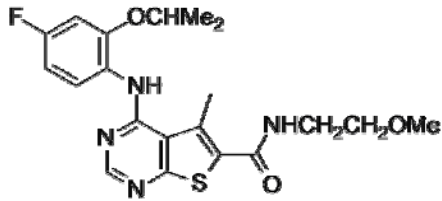
Figure 3. Cell cycle analysis of (A) MOLM-13 and (B) MV4-11 cells after treatment with 5, 10 or 20 μ M of MNKI-19, MNKI-85 or CGP57380 for 24 h and 48 h. Data represent the mean \pm SD of three independent repeats. * p < 0.05 when compared to control. Western blot

analysis of key proteins involved in cell cycle upon treatment with Mnk inhibitors in MOLM-13 cells for (C) 1 h and (D-E) 24 h. In C and D, compounds are tested at 5 μ M and/or 10 μ M and 20 μ M whereas in E, compounds are used at 20 μ M. Antibodies used and the protein molecular weight marker are indicated on the left and right sides, respectively, of each panel. DMSO diluent is used as a control and β -actin is used as an internal loading control. A representative blot is selected from at least two independent repeats.

Figure 4. Induction of apoptosis by MNKI-19, MNKI-85 or CGP57380 in (A) MOLM-13 and (B) MV4-11 cells. Cells are exposed at 5, 10 and 20 μ M of each compound for 24 and 48 h, and examined with Annexin V/PI staining. The percentage of cells undergoing apoptosis is represented by the sum of early and late apoptosis. Data represent the mean \pm SD of three independent repeats. * $p < 0.05$ when compared to control. Western blot analysis of key proteins involved in apoptosis upon treatment with Mnk inhibitors in MOLM-13 cells for (C) 1 h and (D-E) 24 h. In C and D, compounds are tested at 5 μ M and/or 10 μ M and 20 μ M whereas in E, compounds are used at 20 μ M. Antibodies used and the protein molecular weight marker are indicated on the left and right sides, respectively, of each panel. DMSO diluent is used as a control and β -actin is used as an internal loading control. A representative blot is selected from at least two independent repeats. (F) Quantification of caspase-3/7 activity in MOLM-13 (left) and MV4-11 (right) cells upon treatment with 5 μ M, 10 μ M and 20 μ M of MNKI-19, MNKI-85 or CGP57380 for 48 h.

Tables

Table 1. Chemical structure and kinase inhibitory activity of Mnk inhibitors.

<div style="display: flex; justify-content: space-around; align-items: flex-end;"> <div style="text-align: center;">  <p>CGP57380</p> </div> <div style="text-align: center;">  <p>MNKI-19</p> </div> <div style="text-align: center;">  <p>MNKI-85</p> </div> </div>							
K_i (μ M) ^a							
Compound	Mnk1	Mnk2	CDK2A	CDK9T1	CDK4D1	FLT3	Pim-1
CGP57380	1.010 ± 0.098	0.877 ± 0.212	> 10	> 10	> 10	ND	ND
MNKI-19	0.186 ± 0.011	0.068 ± 0.009	> 10	> 10	> 10	> 10	2.35
MNKI-85	> 10	0.031 ± 0.012	> 10	> 10	> 10	> 10	> 10

^aThe ATP concentrations used in these assays were within 15 μ M of K_m . Apparent inhibition constants (K_i) were calculated from IC_{50} values and the appropriate K_m (ATP) values for each kinase using the Cheng-Prusoff equation. Data shown are the mean values derived from two replicates ± SD. ND, not determined.

Table 2. Anti-proliferative activity of CGP57380, MNKI-19 and MNKI-85 in leukemia cell lines with various FLT3 mutational statuses and normal fibroblast cells by 72 h resazurin and MTT assays, respectively.

Cell line	FLT3 status	FAB subtype	72 h GI ₅₀ (μM) ^a ± SD		
			CGP57380	MNKI-19	MNKI-85
MOLM-13	ITD	M5a	8.81 ± 0.80	5.65 ± 0.84	7.19 ± 0.08
MV4-11	ITD	M5	6.89 ± 0.16	7.30 ± 0.75	7.44 ± 0.77
PL-21	ITD/WT	M3	9.39 ± 0.11	57.17 ± 6.74	> 100
HL-60	WT	M2	16.83 ± 1.98	69.18 ± 6.15	> 100
THP-1	WT	M5	38.97 ± 2.98	> 100	94.06 ± 8.40
U937	WT	M4/5	9.40 ± 0.60	33.59 ± 4.21	> 100
K562	WT	(CML)	34.13 ± 1.82	93.16 ± 9.68	> 100
WI-38^b	Normal fibroblast cells		62.37 ± 0.24	98.63 ± 1.54	43.40 ± 5.05

^a Data shown are the mean values derived from at least two replicates ± SD. ^b GI₅₀ values were determined by 72 h MTT assay. FLT3, FMS-like tyrosine kinase-3; ITD, internal tandem duplications; WT, wild-type; FAB, French-American-British classification system.

Figure 1

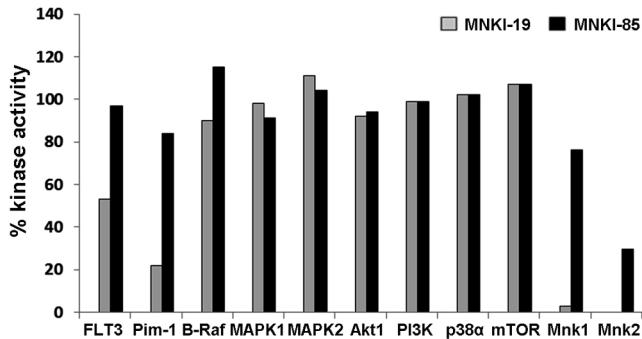


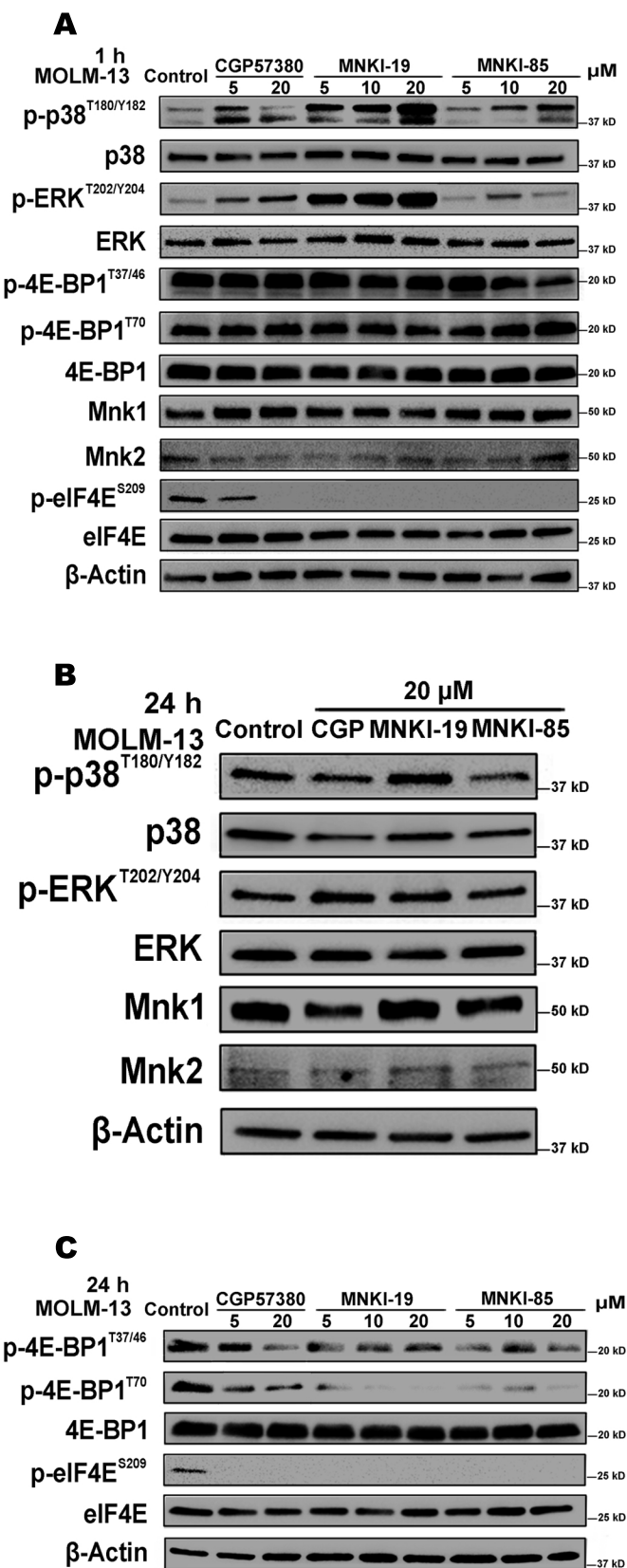
Figure 2

Figure 3

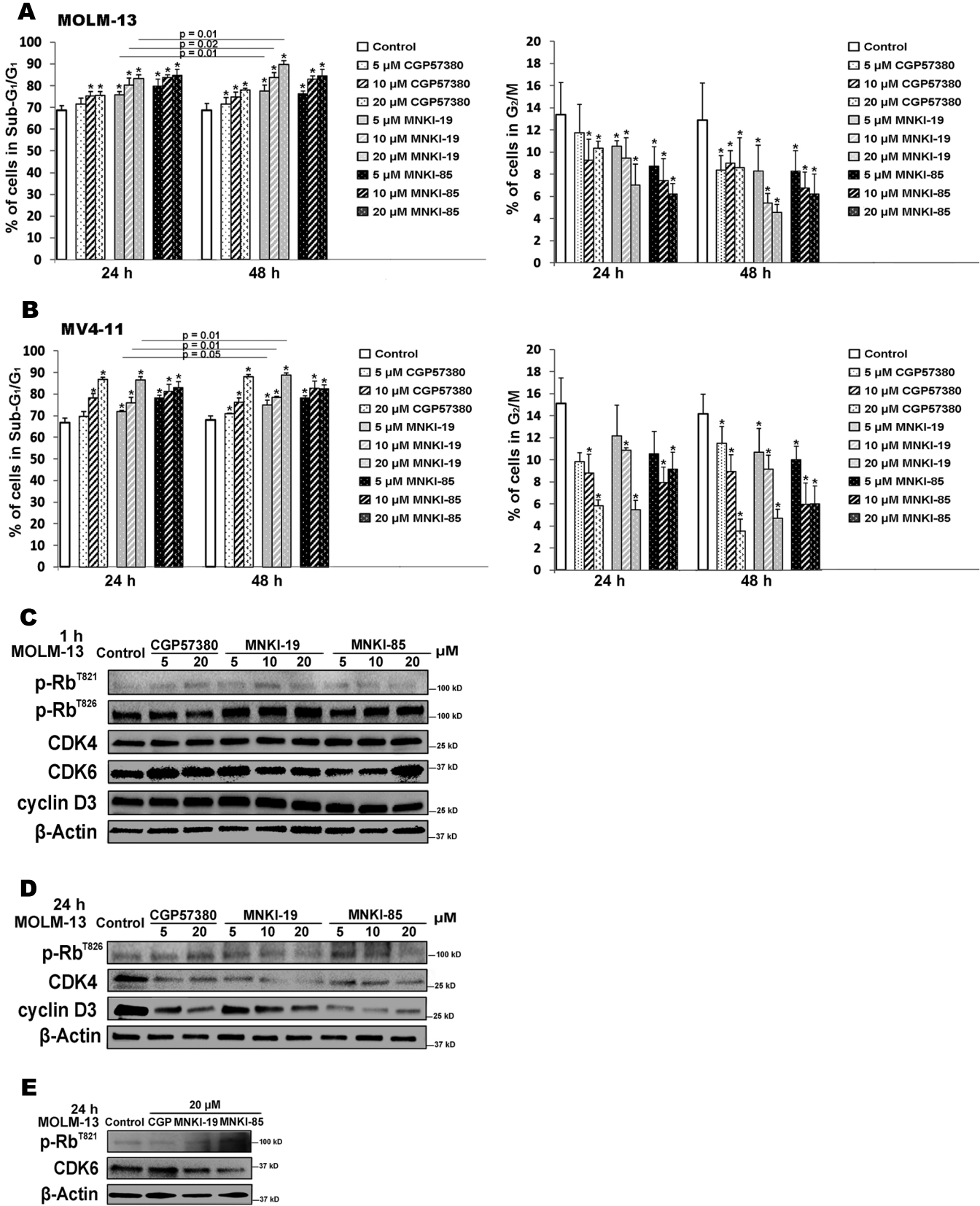


Figure 4